ELSEVIER

Thermochimica Acta 339 (1999) 69–77

thermochimica acta

www.elsevier.com/locate/tca

Thermal behaviour of some dicarboxylic acids and their monoamide derivatives

K. Clou, R. Keuleers, J. Janssens, H.O. Desseyn*

Department of Chemistry, RUCA, University of Antwerp, Groenenborgerlaan 171, 2020 Antwerp, Belgium

Received 17 March 1999; accepted 24 June 1999

Abstract

The thermal behaviour of some dicarboxylic acids and the monoamide derivatives of these acids is studied by the decomposition and the determination of the ΔH and E_a-values.

The differences in these physical constants are explained mainly by the number and strength of the different intermolecular hydrogen bonds. © 1999 Elsevier Science B.V. All rights reserved.

Keywords: Dicarboxylic acids; Hydrogen bonds; Thermal analysis

1. Introduction

The thermal behaviour of solid organic compounds depends mainly on the characteristic intermolecular cohesive forces in the crystal structure. A recent article we published was on the influence of the different types and strengths of hydrogen bonding on the physical behaviour of amides and thioamides [1]. In this article, we focus on molecules exhibiting the carboxylic acid and the amide functional groups.

Carboxylic acids can form hydrogen bonds as they exhibit the O–H proton-donating and the C=O proton-accepting group. The cyclic dimer form is the most frequently observed hydrogen-bond pattern in simple carboxylic acids.

Introducing other possible proton-donating and proton-accepting groups, such as the amide group, in the carboxylic acid molecules gives a variety of possible hydrogen-bond patterns [2]. Among these hydrogen-bond patterns, we can distinguish between the classical acid–acid dimers, acid–acid catamers, and heterogenic associations as given in Fig. 1.

The principal aim of this article is to investigate the thermal behaviour of the different acids and explain the phenomenon by the different hydrogen bonding systems in these molecules. The literature information on the thermal decomposition of the classical dicarboxylic acids is studied by their melting points and decomposition patterns [3,4] without referring to the different hydrogen bonding systems in these molecules. The literature on the thermal behaviour of the monoamide derivatives is practically non-existing as most of the material under investigation consists of original compounds.

2. Experimental

The dicarboxylic acids were obtained from FLUKA (except glutaric acid which was obtained from

---

*Corresponding author.

0040-6031/99/$ – see front matter © 1999 Elsevier Science B.V. All rights reserved.
PII: S0040-6031(99)00195-1

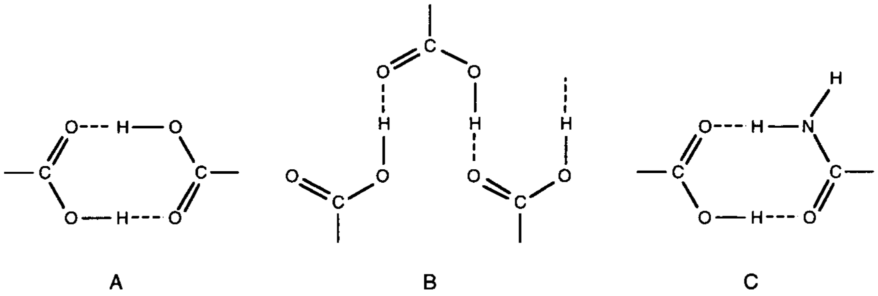

Fig. 1. A: acid–acid dimers; B: acid–acid dimers; C: heterogenic acid–amido dimers.

Aldrich). The compounds were recrystallized from bidistilled water or from C_2H_5OH.

Oxamic acid (Janssen Chimica 0920-4) has been purified by sublimation, and succinamic acid (Aldrich 13.437-6) has been purified by recrystallization from ethanol. Malonamic acid has been prepared according to the literature [5,6].

The oxamic acid derivatives were prepared according to the following scheme:

The compounds formed were purified by recrystallization or sublimation, *N*-methylmalonamic acid was synthesized according to the previous scheme from Potassium-methylmalonamide [7].

N-methylsuccinic acid was prepared from the anhydride by adding CH_3NH_2. *N*-dimethyloxamic acid was prepared according to the previous system by adding $(CH_3)_2NH$ instead of RNH_2 in the first step with oxalate ethylester. The compound was also purified by sublimation.

All compounds under investigation were tested on ^{13}C-NMR spectra.

The infrared spectra were recorded on a Bruker IFS 113 vFT spectrometer. Thermal analysis was performed on TA instruments SDT 2960 TGA 2950 and DSC 2920.

All experiments were performed under dry nitrogen atmosphere (50 ml min^{-1}) and the heating rate was 5°C min^{-1} except when stated otherwise in the text.

3. Results and discussion

3.1. Dicarboxylic acids

All dicarboxylic acids form hydrogen bridges according to the classical dimer type except oxalic acid [3] which is, therefore, not included in the study. The infrared spectra have extensively been studied [3,8]. The nature and the strength of the hydrogen bonding in the solid state can very well be studied through the temperature effect on the fundamentals [9] and the intermonomeric vibrations [10] which are very sensitive to the strength of the hydrogen bonds.

Table 1
The O···O distances in dicarboxylic acids

	Γ (O···O) (pm)	Reference
HOOC–CH_2–COOH (mol)	268	[11]
HOOC–$CHCH_3$–COOH	261	[12]
HOOC–$(CH_2)_2$–COOH (succinamic acid)	266	[13]
HOOC–$(CH_2)_3$–COOH (glutaric acid)	269	[14]
HOOC–$(CH_2)_4$–COOH (adipic acid)	264	[15]

The intermolecular O···O distances in the dimers determine the intermonomeric vibrations and are given in Table 1. These data clearly indicate similar bond strengths in the different molecules. This is also confirmed by the comparable temperature shifts of Acid I, Acid II and Acid V bands as given in Table 2. The comparable positions and shifts also indicate similar hydrogen bond strength in these molecules [8,9].

The melting points given in Table 3 are in close agreement with the literature values. The differences in the melting points are explained by the number of CH_2 groups in the dicarboxylic acids, where a periodic pattern has been observed, depending on the zig-zag structures of these acids [11].

The ΔH values listed in Table 3 represent the total energy involved of the melting, evaporation and decomposition of the acids. This total energy depends

Table 2
The influence of temperature on Acid I, Acid II and Acid V bonds in dicarboxylic acids

	Acid I bond (cm^{-1})			Acid II bond (cm^{-1})			Acid V bond (cm^{-1})		
	20°C	−196°C	Δ	20°C	−196°C	Δ	20°C	−196°C	Δ
HOOC–CH_2–COOH	1705	1701	−5	[a]	[a]		657	662	+5
HOOC–$CHCH_3$–COOH	1701	1697	−4	1426	1433	+7	671	675	+4
HOOC–$C(CH_3)_2$–COOH	1703	1694	−9	1403	1406	+3	666	673	+7
HOOC–$(CH_2)_2$–COOH	1691	1687	−4	[a]	1471		637	642	+5
HOOC–$(CH_2)_3$–COOH	1696	1695	−1	1435	1438	+3	695	698	+3
HOOC–$(CH_2)_4$–COOH	1695	1695	−1	1429	1432	+3	690	692	+2

[a] Not observed due to weak intensity or overlapping bands.

Table 3
ΔH and melting points for some dicarboxylic acids

	ΔH^* (kJ mol^{-1})	$T_{melt.}$	$T_{melt.}$ (4)	$(dm/dt)_{max}$
HOOC–CH_2–COOH	78	136.0	136.0	175
HOOC–$CHCH_3$–COOH	85	135.0	–	172
HOOC–$C(CH_3)_2$–COOH	90	195.0	–	195
HOOC–$(CH_2)_2$–COOH	119	190.2	187.7	209
HOOC–$(CH_2)_3$–COOH	116	99.2	98.5	220
HOOC–$(CH_2)_4$–COOH	115	153.3	153.4	236

strongly on the crystal structure and the intermolecular hydrogen bonds. From the infrared spectra, we could clearly show that the intermolecular hydrogen bonds are very similar and of equal strength [8]. So the difference between the malonic acids and the higher dicarboxylic acids must mainly be due to the crystal structure. Indeed, the malonic acids belong to the triclinic system, whereas the other acids exhibit a monoclinic system.

Fig. 2 gives the TG and DTA curves for malonic acid (A), methylmalonic acid (B) and dimethylmalonic acid (C). Malonic acid exhibits a phase transition around 100°C. This transition energy is calculated at about 4 kJ mol^{-1}. X-ray analysis [14] and vibrational spectra also prove this reversible phase transition. The loss of weight of dimethylmalonic acid occurs in one endothermic process at a speed of 5°C min^{-1}, as can be observed from Fig. 3C.

Fig. 3 gives the DSC curves for dimethylmalonic acid at different heating rates; the data are given in Table 4. At very low heating rates, the compound is already sublimed before the melting point; at

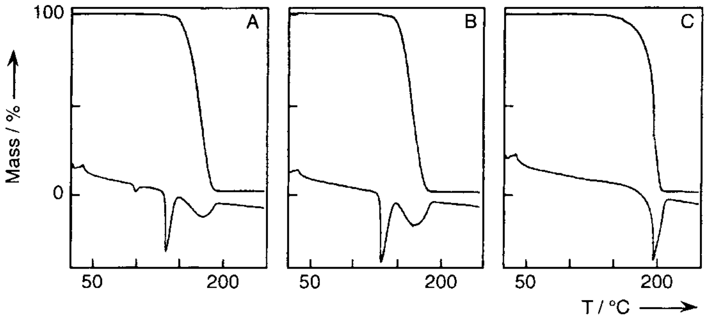

Fig. 2. TG and DTA curves for malonic acid (A), methylmalonic acid (B) and dimethylmalonic acid (C).

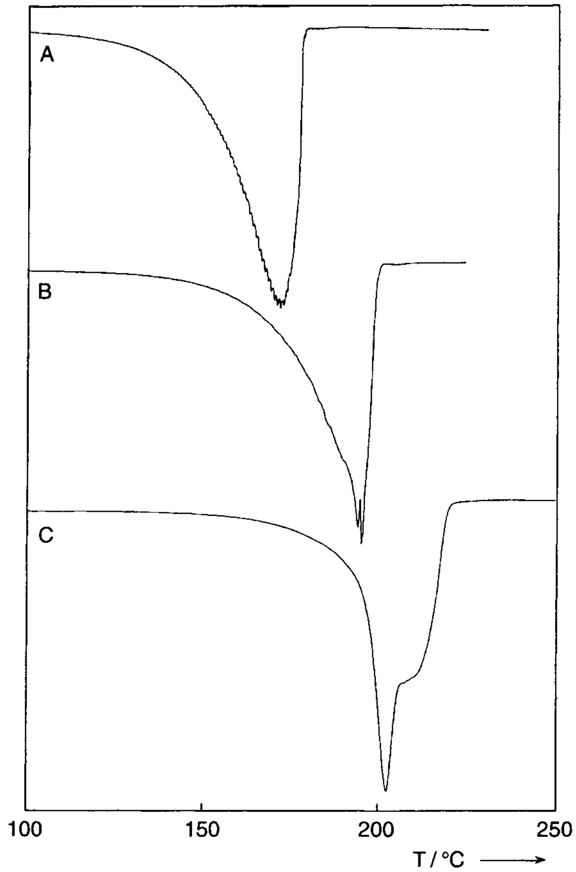

Fig. 3. DSC curves for dimethylmalonic acid at 1°C min^{-1} (A), 5°C min^{-1} (B) and 20°C min^{-1} (C).

5°C min^{-1}, we observed a melting of the rest at about 195.5°C. At higher heating rates, we clearly observe the start of the sublimation (as controlled by the TGA curves) a clear melting and boiling and/or decomposition of the acid. The decomposition of the compound at higher heating rates is clear from the higher ΔH values obtained for these processes.

Table 4
Thermal data for dimethylmalonic acid at different heating rates

(°C min^{-1})	$T_{\mathrm{melt.}}$ (°C)	$T_{\mathrm{subl.}}$ (°C)	$\Delta H_{\mathrm{Total}}$ (kJ mol^{-1})
1		171	94.9
2		182	94.2
5	195.5	195.5	92.2
10	198		104
20	202		103

All the dicarboxylic acids under investigation exhibit a sharp endothermic peak due to the melting followed by a broad endothermic band indicating the boiling and/or decomposition of the compound. The $(dm/dt)_{\max}$ values, as given in Table 3, increase as expected with increasing mass of the compounds, indicating rather a boiling process than a decomposition process.

A typical example is given for glutaric acid in Fig. 4; from Fig. 4, we can also observe a phase transition at 71°C ($\Delta H = 4$ kJ mol^{-1}).

3.2. Oxamic acid, malonamic acid, succinamic acid

Oxamic acid behaves as a hydrogen bonded polymer with cyclic acid–acid and cyclic amide–amide dimers [16,17,18]. This typical pattern is given in Fig. 5.

Cyclic acid–amide intermolecular associations occur in succinamic acid [2] and are given in Fig. 6. Malonamic acid has only been studied by

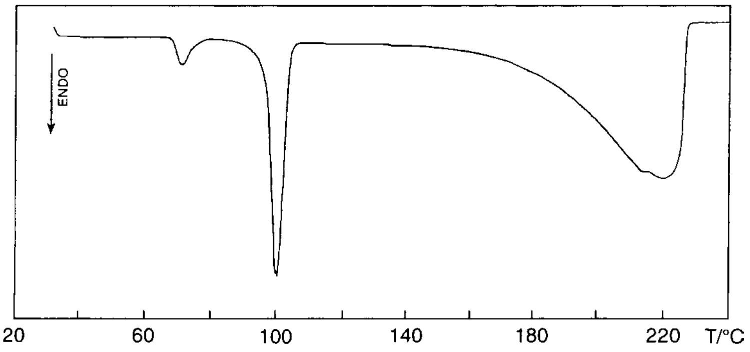

Fig. 4. DTA curve for glutaric acid, showing the phase transition, melting and boiling processes.

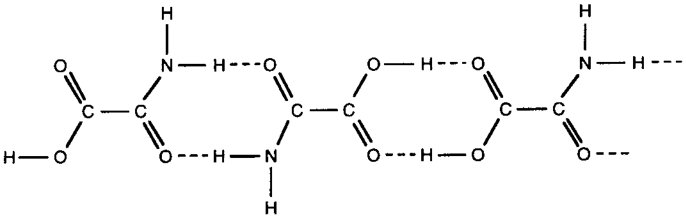

Fig. 5. The hydrogen bonding pattern in oxamic acid.

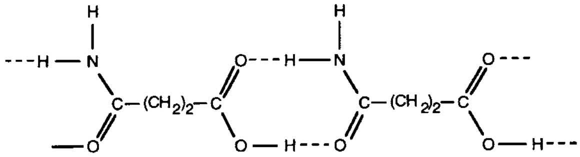

Fig. 6. The hydrogen bonding pattern in succinamic acid.

vibrational spectroscopy [18] and the strong resemblance with the spectra of succinamic acid lets us suggest a similar structure.

As malonamic acid exhibits the typical behaviour of α-ketosubstituted carbonic acids, we observed a decomposition at 150°C according to the following reaction:

$$\mathrm{HOOC{-}CH_2{-}CONH_2} \xrightarrow{150^{\circ}\mathrm{C}} \mathrm{CH_3{-}CONH_2} + \mathrm{CO_2}$$

The different structures and the fact that malonamic acid decomposes make a comparison of the temperature and the energy for these different compounds unrealistic. These data are scheduled in Table 5; Table 5 also contains the data for the methylderivatives. These compounds exhibit lower sublimation, melting and boiling points and also lower ΔH values. This can very well be explained by assuming less of hydrogen bonds in the secondary amide compound compared to the primary amide groups.

From Table 5, we can also explain the series oxamic acid, *N*-methyloxamic acid and *N*-dimethyloxamic acid. The ΔH values clearly indicate the importance of the number of hydrogen bonds as we observed the highest values for oxamic acid, with three possible hydrogens involved in intermolecular hydrogen bonds, compared to two for the methyl derivative and one hydrogen of the disubstituted derivative.

Fig. 7 shows the DSC curves for dimethyloxamic acid; the data are given in Table 6. The total process changes from pure sublimation at 0.25°C min^{-1} to a melting and boiling process at 20°C min^{-1}. The ΔH values are very well comparable, indicating the same process, i.e. the transition from the solid state to the gas phase.

3.3. N-alkyloxamic acids

N-alkyloxamic acids exhibit different crystal structures, depending on the alkyl substituent and the temperature [19]. The vibrational spectra are, for the different structures, very characteristic and can be classified into two different modifications, called the α and γ structures [19].

Table 5
Thermal data for some amide derivatives of dicarboxylic acids

	T_{onset} (sublimation)	$T_{\mathrm{melt.}}$	$(\mathrm{d}m/\mathrm{d}t)_{\mathrm{max}}$	ΔH
$\mathrm{H_2NCOOH}$	191			119
$\mathrm{CH_3HNCOCOOH}$ (α)	130			94.3
$\mathrm{(CH_3)_2NCOCOOH}$		130	137	72.2
$\mathrm{H_2NCOCH_2COOH}$		117	150	82
$\mathrm{CH_3HNCOCH_2COOH}$		103	142	78
$\mathrm{H_2NCO(CH_2)_2COOH}$		158	190	137[a]
$\mathrm{CH_3HNCO(CH_2)_2COOH}$		113	175	103[a]

[a] Decomposition.

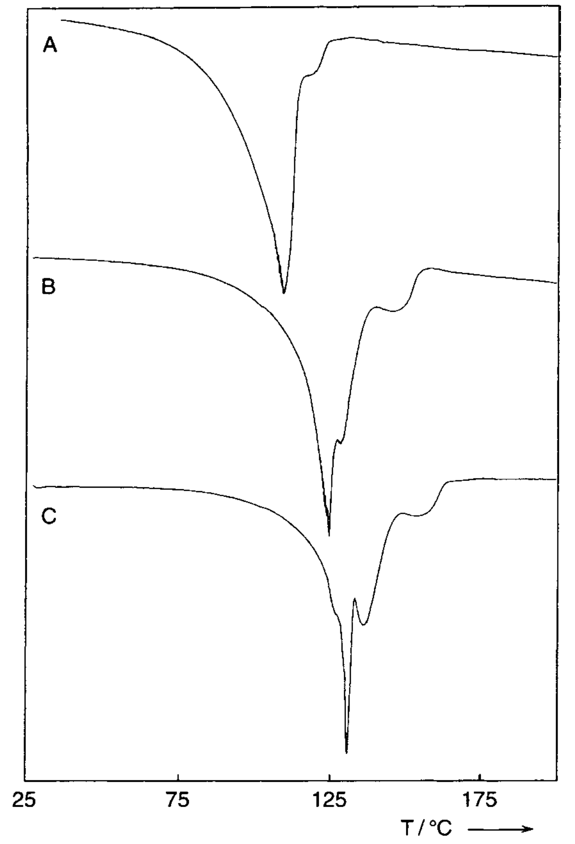

Fig. 7. DSC curves for dimethyloxamic acid at 0.25°C min^{-1} (A), 5°C min^{-1} (B) and 20°C min^{-1} (C).

Table 6
Thermal data for dimethyloxamic acid at different heating rates

(°C min^{-1})	$T_{\mathrm{melt.}}$ (°C)	$T_{\mathrm{boil.}}$ (°C)	$\Delta H_{\mathrm{Total}}$ (kJ mol^{-1})
0.25	109		72.2
2	124	128	71.4
5	130	137	72.2
20	137	154	73.2

Table 7
Thermal data for *N*-alkyloxamic acids (RHNCOCOOH)

R=		ΔH (kJ mol^{-1})	$(\mathrm{d}m/\mathrm{d}t)_{\mathrm{max}}$	T_{trans}	$\Delta H_{\mathrm{trans}}$
CH_3	α	94.1	130		
	γ	89.8	128		
C_2H_5	γ	99.7	132	49.1	2.8
C_3H_7	γ	98.7	137	43	2.6
iC_3H_7	γ	90.2	125		
cC_3H_5	α	90.2	141	92	0.6
				102	0.9
				138	1.3
C_4H_9	γ	112	147		
iC_4H_9	γ	109	125		
cC_5H_9	α	114	152		

The thermal data are, for different compounds, given in Table 7. Some products exhibit both structures at room temperature, whilst others exhibit only the second structure at higher temperatures.

Both the α and γ structures are stable at room temperature for the methyl derivative. Fig. 8 shows the TG, DTA and DSC curves for the α compound; no endothermic process, indicating the transition to the γ structure, is observed probably due to the fact that this transition occurs at higher temperature and the weak

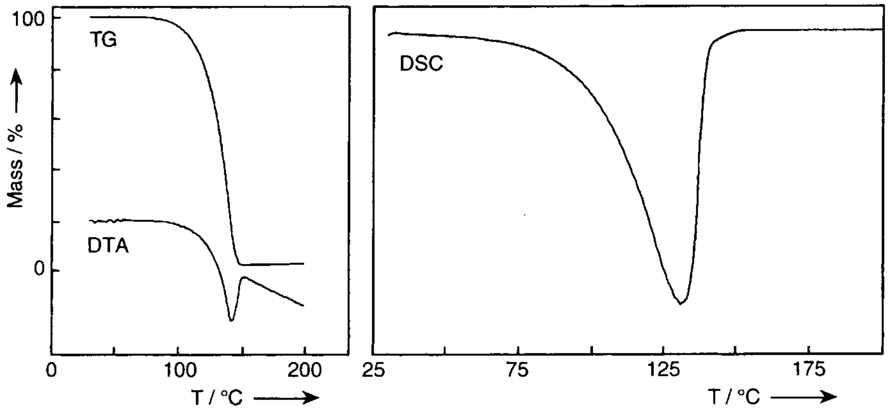

Fig. 8. TG, DTA and DSC curves for α-*N*-methyloxamic acid.

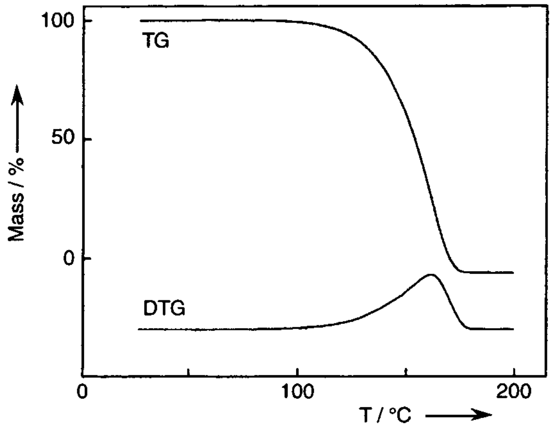

Fig. 9. TG and DTG curves for *N*-cyclopropyloxamic acid.

endothermic signal is then overlapped by the intense endothermic process of sublimation. The Δ*H* values and the $(dm/dt)_{max}$ are, for both structures, given in Table 7. The difference of about 4 kJ mol^{-1} must mainly be ascribed to the difference in hydrogen bonding in both structures. Also, the slightly higher $(dm/dt)_{max}$ for the α compound is an indication of the stronger intermolecular forces in the α structure.

The most significant example of this series is the cyclopropyl derivative. The TG, DTG and DSC curves at, respectively, 0.25 and 5°C min^{-1} are given in Figs. 9 and 10. The TG and especially the DTG curves give an asymmetric profile indicating different processes. These different processes are clear from the DSC curve where the sublimation process starts already at a very low temperature, and phase transitions are observed at 91.3, 103.5 and 138.2°C followed by the melting process at 147°C and the evaporation of the compound at 188°C. So the loss of weight consists of sublimation over the whole temperature range and the evaporation at higher temperature.

Fig. 10 shows the DSC curve at 0.25°C min^{-1}; from Fig. 10, we clearly observe the first phase transition at 92°C and the sublimation process with T onset at 115°C.

The shoulder on the high temperature side of the sublimation curve is the melting process of the rest of the compound. The higher Δ*H* value obtained at 5°C min^{-1} (90.2 kJ mol^{-1} compared to 84.0 kJ mol^{-1} at 0.25°C min^{-1}) indicates that there is probably also some decomposition of the compound at about 200°C. This decomposition can be expected for these carbo-

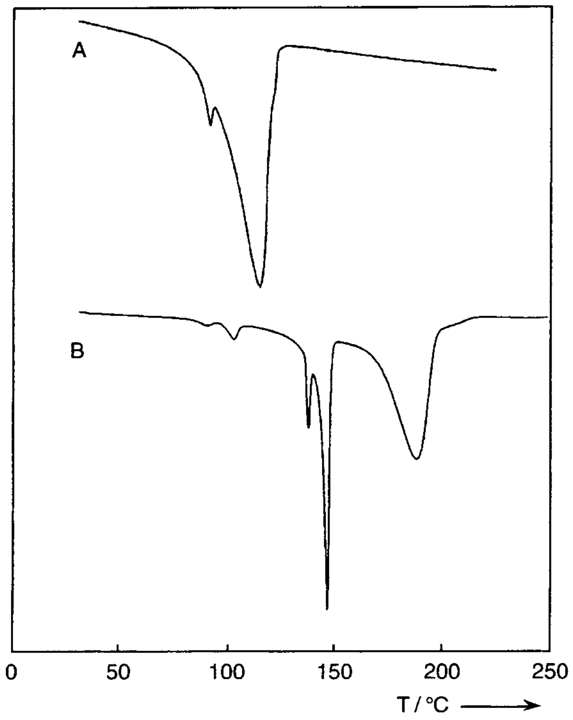

Fig. 10. DSC curves for *N*-cyclopropyloxamic acid at 0.25°C min^{-1} (A) and 5°C min^{-1} (B).

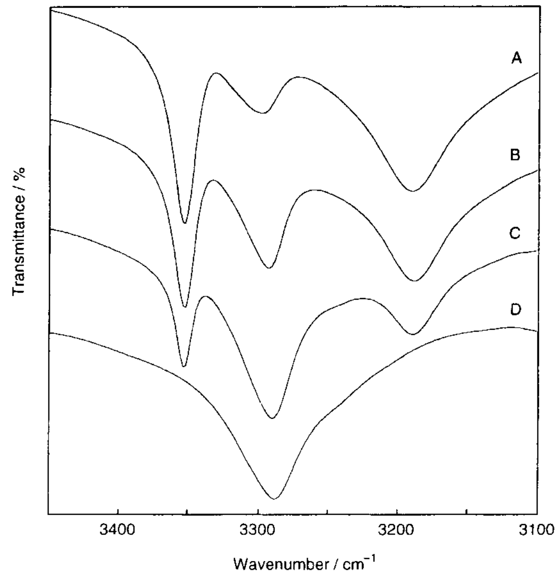

Fig. 11. The νNH and νOH region of *N*-cyclopropyloxamic acid at increasing temperature from A (lowest temperature) to D (highest temperature).

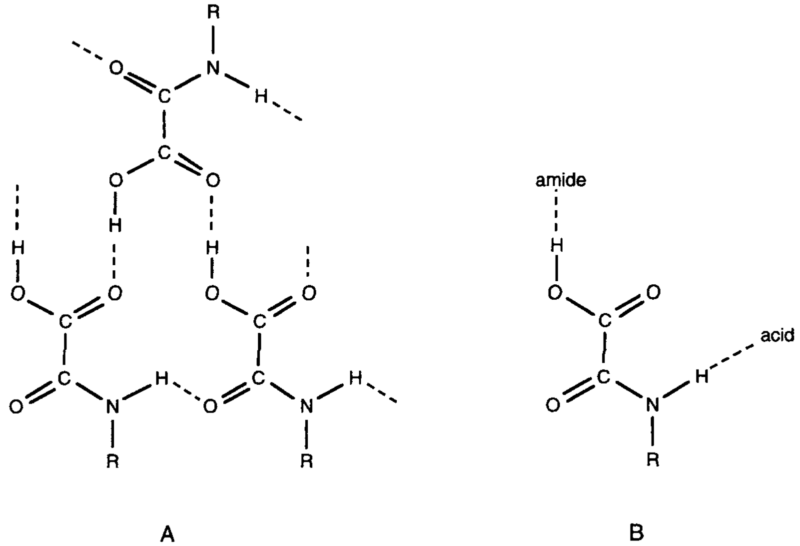

Fig. 12. The α and γ hydrogen bonding patterns in *N*-alkyloxamic acids.

nic acids. The phase transitions of about 3 kJ mol^{-1} are due to the different hydrogen bond systems in the solid compound. The difference in this intermolecular hydrogen bond system is obvious from the infrared spectra at different temperatures given in Fig. 11.

The amide–amide νNH band and the acid–acid catamer νOH band appear as well separated bands at, respectively, 3353 and 3189 cm^{-1} for the α-modification at room temperature. At higher temperatures, these bands disappear and a broad band at about 3291 cm^{-1} with overlapping νNH and νOH modes appears as a characteristic for the γ modifications where we observe the acid–amide νNH and νOH modes. The different patterns are given in Fig. 12.

The νNH modes become more strongly hydrogen bonded and the νOH modes are less hydrogen bonded in the γ structure. The total energy involved in this $\alpha \rightarrow \gamma$ transition is about 3 kJ mol^{-1} and is a good measure for the difference in the hydrogen bonding strength between the α and γ modifications.

Acknowledgements

The authors thank the FWO for TA instrumentation. R. Keuleers thanks the FWO for the obtained grant. The authors also thank G. Thijs for technical assistance.

References

[1] S.H.J. De Beukeleer, J.F. Janssens, H.O. Desseyn, J. Therm. Anal. 48 (1997) 225.
[2] L. Leisterowitz, Acta Cryst. B 32 (1976) 775.
[3] Y. Suzuki, K. Muraishi, K. Matsuki, Thermochim. Acta 211 (1992) 171.
[4] K. Muraishi, Y. Suzuki, Thermochim. Acta 232 (1994) 195.
[5] I. Jeffery, L. Vogel, J. Am. Chem. Soc. 56 (1934) 1102.
[6] D. Galat, J. Chem. Soc. London 70 (1948) 2596.
[7] A. Kende, Organic Synthesis, vol. 64, Wiley, NY, 1986, p. 144.
[8] I. Wolfs, H.O. Desseyn, Appl. Spectrosc. 50 (1996) 1000.
[9] B. Slootmaekers, H.O. Desseyn, Appl. Spectrosc. 45 (1991) 118.
[10] Y. Maréchal, A. Witkowski, J. Chem. Phys. 48 (1968) 3697.
[11] J.A. Goedkoop, C.H. McGillavry, Acta Cryst. 10 (1957) 125.
[12] J.L. Derissen, Acta Cryst. B 26 (1970) 901.
[13] J.S. Broadly, D.W.J. Gruickshank, J.D. Morrison, J.M. Robertson, H.M.M. Shearer, Proc. R. Soc. London A 251 (1959) 441.

[14] J.D. Morrison, J.M. Robertson, J. Chem. Soc. 1949 (1949) 1001.
[15] J. Housty, M. Hospital, Acta Cryst. B 26 (1970) 901.
[16] J. Villepin, M.H. Limage, A. Novak, N. Toupy, M. Lepostallec, H. Poulet, S. Ganguly, C.N.R. Rao, J. Raman Spectrosc. 15 (1984) 41.
[17] G.N.R. Tripathi, J.E. Katon, Spectrochim. Acta 35A (1979) 401.
[18] I. Wolfs, H.O. Desseyn, Spectrochim. Acta 51A (1995) 1601.
[19] I. Wolfs, H.O. Desseyn, Spectrochim. Acta A 52A (1996) 1521.